

PCCP

Accepted Manuscript



This is an *Accepted Manuscript*, which has been through the Royal Society of Chemistry peer review process and has been accepted for publication.

Accepted Manuscripts are published online shortly after acceptance, before technical editing, formatting and proof reading. Using this free service, authors can make their results available to the community, in citable form, before we publish the edited article. We will replace this *Accepted Manuscript* with the edited and formatted *Advance Article* as soon as it is available.

You can find more information about *Accepted Manuscripts* in the [Information for Authors](#).

Please note that technical editing may introduce minor changes to the text and/or graphics, which may alter content. The journal's standard [Terms & Conditions](#) and the [Ethical guidelines](#) still apply. In no event shall the Royal Society of Chemistry be held responsible for any errors or omissions in this *Accepted Manuscript* or any consequences arising from the use of any information it contains.

Splitting and Joining in Carbon Nanotube/Nanoribbon/Nanotetrahedron Growth

Takayuki Hasegawa^a, and Hideo Kohno^{*b}

Received Xth XXXXXXXXXXXX 20XX, Accepted Xth XXXXXXXXXXXX 20XX

First published on the web Xth XXXXXXXXXXXX 200X

DOI: 10.1039/b000000x

We report a novel phenomenon in carbon nanotube growth that results in a new carbon nanotube morphology. A carbon nanotube grown via metal nanoparticle-catalyzed chemical vapor deposition splits into two flattened nanotubes during growth and the two flattened nanotubes merge to form a ring of carbon nanotube/nanoribbon. This novel process is revealed with transmission electron microscopy observations of the carbon nanostructures. We propose that the splitting-and-joining process involves only one metal catalyst nanoparticle and a self-folding mechanism that we have named the origami mechanism to explain the process and the formation of nanoribbons and nanotetrahedra.

Branching in carbon nanotube (CNT) growth was first reported by Zhou and Seraphin¹, where CNTs grown by carbon arc-discharge appeared to have horn-like projections in three directions. This novel phenomenon aroused interest in the fundamental aspects of catalytic CNT growth and opened up new possibilities of CNT application to various devices and to nanowiring. After this discovery, many groups reported the formation of Y-branched (Y-junction) and multi-branched CNTs prepared using various methods. The most standard methods employed for the fabrication of branched CNTs are pyrolysis and catalytic chemical vapor deposition (CVD)^{2–11}. Four different formation processes for branched CNTs have been identified in these studies. (i) Several CNTs can grow simultaneously from a catalyst metal nanoparticle or sequentially. (ii) A catalyst metal nanoparticle moves back into the formed CNT and a branch is formed. (iii) A catalyst metal nanoparticle is broken into fragments and each forms a branch. (iv) Catalyst nanoparticles are attached onto the surface of a trunk CNT and each catalyst particle forms a branch. There are two other methods for the fabrication of branched CNTs; welding^{12–15} and the use of templates^{16–18}. These two methods/modes are not directly related to the fundamental aspects of metal-nanoparticle-catalyzed CNT growth; therefore, they are not discussed in detail here.

In the metal-nanoparticle-catalyzed growth by these four modes, branches are always formed from the CNT trunk. Only

one exception can occur when the catalyst metal nanoparticle of a CNT makes arbitrary contact with another distinct CNT or catalyst metal nanoparticle and these two CNTs then merge into one¹⁵. In this paper, we report a novel phenomenon in the metal-nanoparticle-catalyzed growth of multi-walled CNTs, where a CNT grown from a catalyst metal nanoparticle splits into two flattened CNTs (nanoribbons) that continue to grow simultaneously from the metal nanoparticle, followed by joining of the two nanoribbons to form a single tubular or flattened CNT. This results in the formation of a closed loop. The origin of CNT splitting is attributed to a mechanism we have named the origami mechanism, in which a CNT that is expelled from a metal nanoparticle is forced to be flattened in two opposing directions^{19,20}.

Figure 1 shows transmission electron microscopy (TEM) images of a carbon nanotube nanostructure that is split and joined²¹. In this study, the carbon nanostructures were fabricated via a simplified CVD process. Firstly, 0.5 mg hexadecanoic acid [C₁₅H₃₁COOH] and a SiO₂ substrate on which a 20 nm thick layer of Fe is deposited are sealed in an evacuated silica tube (inner diameter = 6 mm, ca. 12 cm long). The sample is then heated at 1000 °C for 30 min to allow for CNT growth. In the example shown in Fig. 1, two splitting and joining events are evident. The left end is a CNT without a metal catalyst nanoparticle; therefore, this part was grown first. The width of the CNT was narrowed from left to right due to flattening, and it collapses fully near the position indicated by the arrow in Fig. 1b. The CNT splits into two nanoribbons, which are then joined together to form a nanotube (Fig. 1c), split into two nanoribbons again (Fig. 1d), and

^a Graduate School of Science, Osaka University, Toyonaka, Osaka 560-0043, Japan.

^b Department of Environmental Science and Engineering, Kochi University of Technology, Kami, Kochi 782-8502, Japan. E-mail: kohno.hideo@kochi-tech.ac.jp

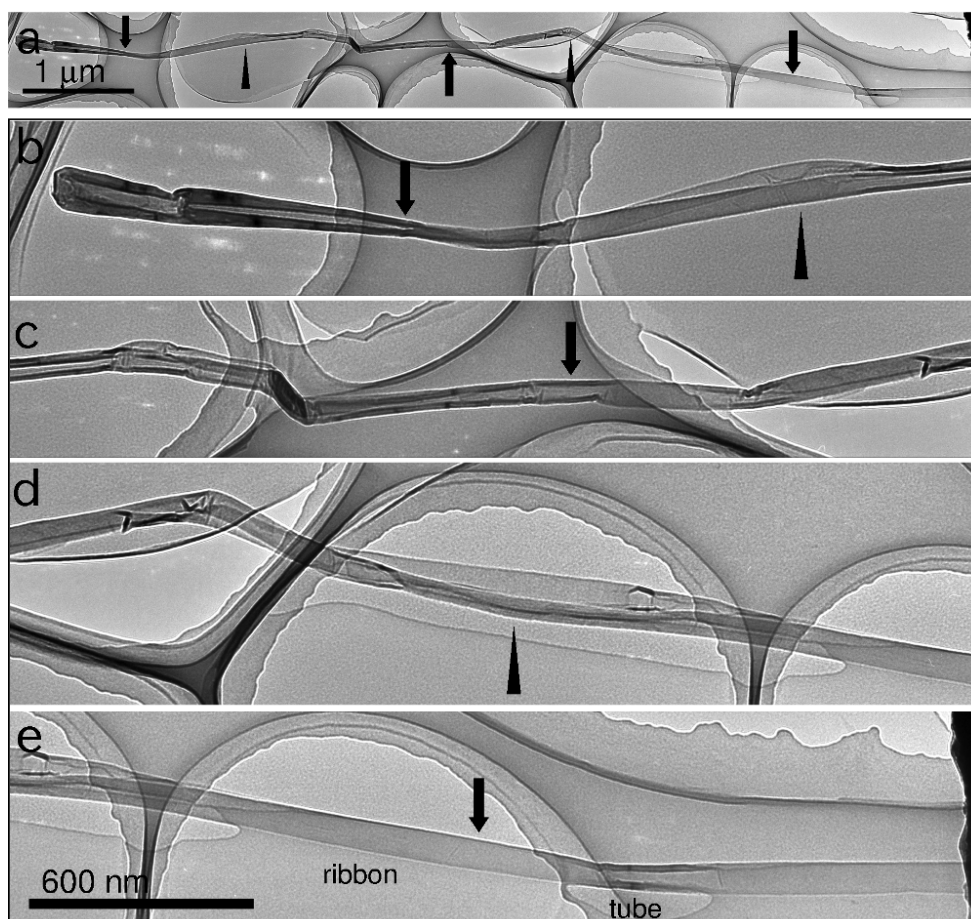


Fig. 1 TEM images of splitting and joining of a CNT structure. (a) Overall view and (b)-(e) details shown in four enlarged images. The arrows and arrowheads indicate the positions of the parts of a single nanotube/nanoribbon and the parts of split nanoribbons, respectively.

finally merged into a nanoribbon/nanotube at the right end of the TEM image (Fig. 1e). From the tubular part in Fig. 1e, the CNT had approximately 60 walls, and the widths of the tubular and flattened parts in Fig. 1e were measured to be 65 nm and 82 nm, respectively. The tubular and flattened parts can be distinguished by the clearer contrast at the edges.

Another example of a splitting and joining structure was identified using electron microdiffraction analysis, as shown in Fig. 2. This example also shows that the split part is composed of two nanoribbons that merge into a nanotube at both ends. The electron diffraction pattern from the two nanoribbons after splitting indicates that they have the armchair-type structure, in accordance with our previous report on flattened nanotube formation via the origami mechanism^{19,20}. It should be noted that the two nanoribbons have almost the same crystal orientation.

To examine the possibility that two independent nanotubes/nanoribbons are simply attached side by side, a split-

and-joined structure with tubular ends was viewed along three different directions by rotating the sample to provide three TEM images with different aspects (Fig. 3). The split parts are nanoribbons again in this example, and they merge into a nanotube at both ends. This observation confirms that the tubular parts at both ends actually consist of individual multi-walled nanotubes. In addition, nanotetrahedra (indicated by the arrows) were identified around the junctions at the split parts of the nanoribbons.

A possible process for the formation of the split into two nanoribbons is unzipping of the nanotube^{22–26}. If two sides of a nanotube are unzipped, then the nanotube is split into two nanoribbons. Nanoribbons formed via this process have literal edges, where the periodic arrangement of carbon atoms is terminated; however, high-resolution TEM analysis revealed that the edges of the present split nanoribbons have graphitic lattice fringes, as shown in Fig. 4. These fringes are characteristic of flattened multi-walled carbon nanotubes, and unzipped

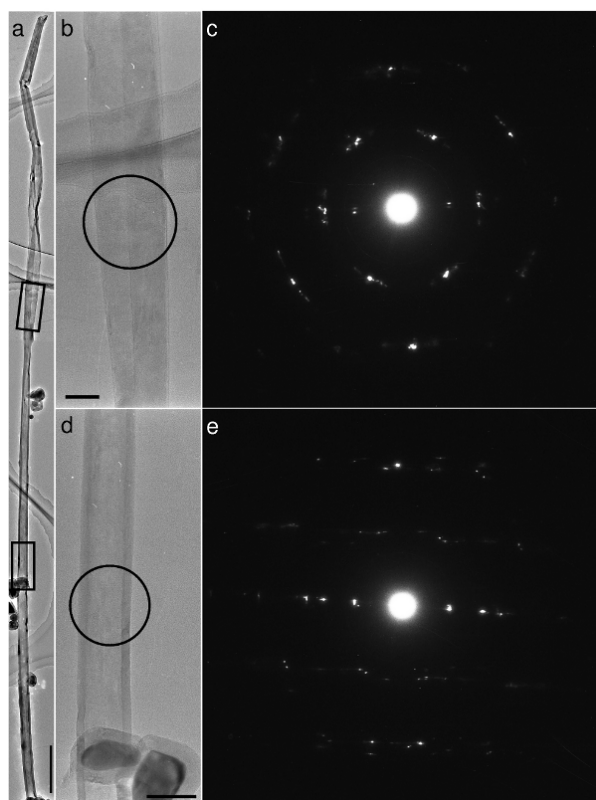


Fig. 2 (a) Overall TEM image of a carbon nanotube structure with splitting and joining. (b) Enlarged image of the area indicated by the upper rectangle in (a) where the nanotube is split into two nanoribbons, and (c) electron diffraction pattern of this part. (d) Enlarged image of the area indicated by the lower rectangle in (a), and (e) electron diffraction pattern of this part. Scale bars are 500 nm in (a) and 100 nm in (b) and (d).

nanoribbons do not show such lattice fringes. Therefore, the high-resolution TEM image provides evidence that the flattened nanotubes were formed. The smooth and straight edges of the split nanoribbons also support this because unzipping of the nanotube typically results in rugged edges.

Based on TEM observations of the split-and-joined structures, we suggest the following model for this phenomenon (Fig. 5). When flattening of the nanotube in one direction is more extreme than that in the other direction, simple flattening occurs and results in the formation of a nanoribbon (Fig. 5a). However, when flattening occurs equally in the two orthogonal directions, it results in the formation of pleats and the nanotube will take an X-shape (Fig. 5b, also see c). If the pleats meet, then it is possible that they reconstruct the structure to form two nanoribbons (flattened nanotubes). Finally, if the two split nanoribbons meet, then they can merge into a nanotube or nanoribbon via the reverse process of splitting.



Fig. 3 TEM image of a split-and-joined structure viewed along three different directions (-40° , 0° , and 40°). Nanotetrahedra are indicated by arrows.

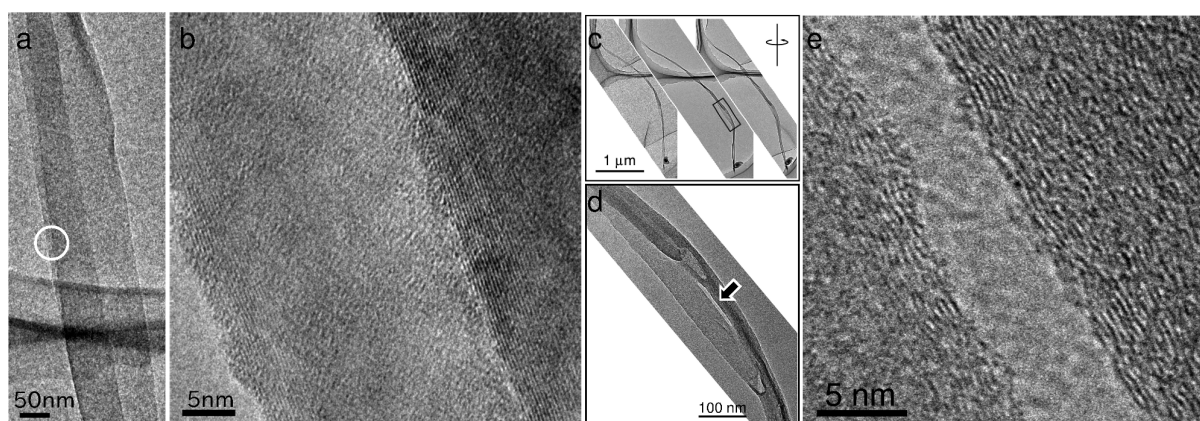


Fig. 4 (a) TEM image and (b) high-resolution TEM image of the split nanoribbons shown in Fig. 3. (c) TEM images of another structure viewed along three directions ($-40, 0, 39^\circ$). (d) Enlarged image of a slit (indicated by the arrow), and (e) high resolution TEM image of the area around the slit showing lattice fringes at the edges.

The joining process can be explained as follows. Owing to the origami mechanism, the two flattened nanoribbons are forced to converge again, and the nanoribbons adhere to each other. Driven by the adhesive force between the two nanoribbons, the roots of the nanoribbons are also forced to converge, and then they join.

Figs. 5d and e show TEM images of CNTs, in which dark lines which originate from the inner walls of CNTs run toward inside diagonally. These image can be explained well if the CNTs have X-shaped cross-section as shown in Fig. 5b. In this model, the split parts of the nanotube have a tendency to become flattened, which is consistent with our TEM observations, where most of the split parts were nanoribbons (flattened nanotubes). Some nanotetrahedra were observed near junctions at the split parts of the nanoribbons (see Fig. 3 and Fig. 4d). The formation of these nanotetrahedra is caused by the instability of the flattening during the origami mechanism, when the flattening works equally in the two directions. This opposed flattening equally matched in strength can also induce complex flattening, as shown in Fig. 5b, and splitting. Therefore, it is reasonable that nanotetrahedra are formed around the junctions. The electron diffraction pattern obtained from the split nanoribbons in Fig. 3c also supports this model because the two split nanoribbons had almost the same crystal orientation (armchair type). This indicates that the two split nanoribbons have the same origin, i.e., they originate from the same single nanotube.

We examined several hundreds of carbon nanostructures grown by our method, and found that 1.3 % of them have the splitting and joining structure. We also found most of the splitting accompanies with joining in most cases. We speculate some additional impurity triggers the phenomenon, and the joining is nearly inevitable after it splits.

In conclusion, the splitting-and-joining phenomenon during metal-catalyzed CNT growth was investigated. The results obtained provide a route for the formation of CNTs with novel morphology. TEM observations revealed details of the structure and suggest that the novel nanostructures are most likely formed by a self-folding mechanism that we have called the origami mechanism. As a result of the splitting-and-joining phenomenon, O-shaped CNTs were formed. In other words, slits were formed in the CNTs. Future research will include control of the splitting-and-joining phenomenon to realize a chain formation of slits, and to reduce the wall number to one or two and control the diameter/width of the resultant nanostructures.

Acknowledgments

This work was supported in part by the Adaptable and Seamless Technology Transfer Program through Target-driven R&D of the Japan Science and Technology Agency. The authors thank S. Ichikawa for support.

References

- 1 D. Zhou and S. Seraphin, *Chem. Phys. Lett.*, 1995, **238**, 286–289.
- 2 B. C. Satishkumar, P. J. Thomas, A. Govindaraj and C. N. R. Rao, *Appl. Phys. Lett.*, 2000, **77**, 2530.
- 3 O. T. Heyning, P. Bernier and M. Glerup, *Chem. Phys. Lett.*, 2005, **409**, 43–47.
- 4 F. L. Deepak, A. Govindaraj and C. N. R. Rao, *Chem. Phys. Lett.*, 2001, **345**, 5.
- 5 W. Z. Li, J. G. Wen and Z. F. Ren, *Appl. Phys. Lett.*, 2001, **79**, 1879.
- 6 B. Gan, J. Ahn, Q. Zhang, S. F. Yoon, Rusli, Q.-F. Huang, H. Yang, M.-B. Yu and W.-Z. Li, *Diam. Relat. Mater.*, 2000, **9**, 897–900.

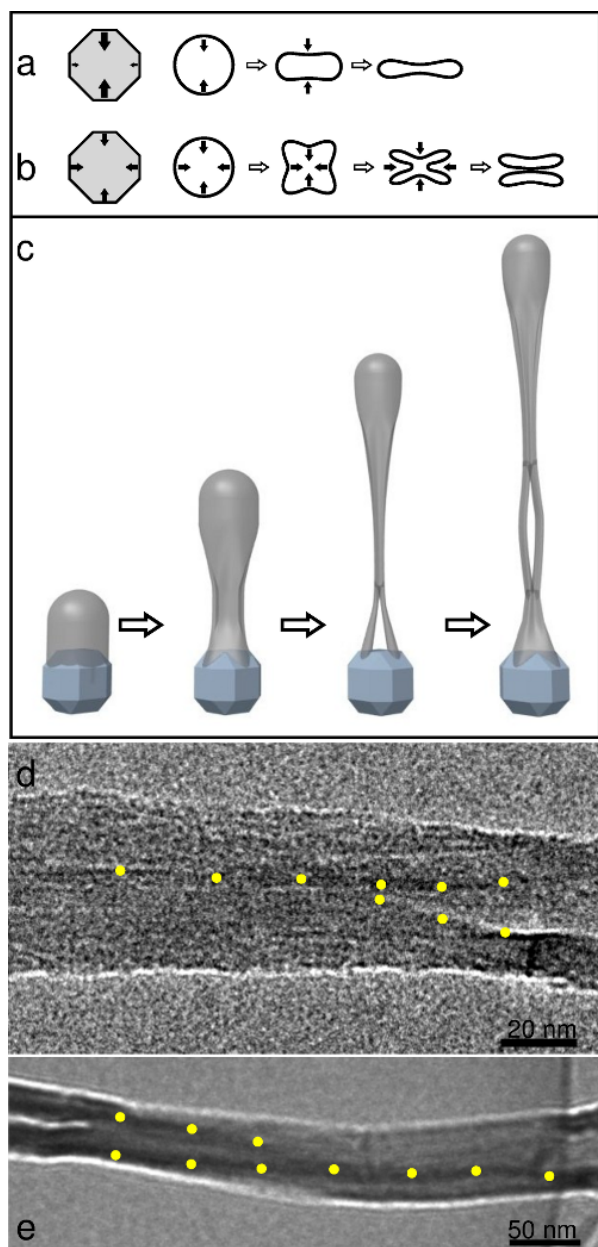


Fig. 5 (a-c) Schematic illustration of the proposed formation mechanism. The gray and white areas represent catalyst metal nanoparticles and the CNTs, respectively. (a) One of two flattening directions is superior when a nanotube is expelled from a metal catalyst nanoparticle, which results in the formation of a simple nanoribbon (flattened nanotube). (b) Flattening occurs equally in both directions, which results in X-shaped folding and splitting. Viewed along the growth direction in (a) and (b). (c) A nanotube grown from a metal nanoparticle splits into two nanoribbons due to the process shown in (b), and then join together via the reverse process. As a result, an O-shaped carbon nanotube is formed. (d) and (e) TEM images of CNTs with X-shaped cross-section. (e) is a part of Fig. 1(b).

- 7 L. F. Su, J. N. Wang, F. Yu and Z. M. Sheng, *Chem. Vap. Deposition*, 2005, **11**, 351–354.
- 8 X. Tao, X. Zhang, J. Cheng, Y. Wang, F. Liu and Z. Luo, *Chem. Phys. Lett.*, 2005, **409**, 89–92.
- 9 J.-M. Ting, T.-P. Li and C.-C. Chang, *Carbon*, 2004, **42**, 2997–3002.
- 10 H. Zhu, L. Ci, X. Xu, J. Liang and S. Wu, *Diam. Relat. Matter.*, 2002, **11**, 1349.
- 11 N. Gothard, C. Daraio, J. Gaillard, R. Zidan, S. Jin and A. M. Rao, *Nano Lett.*, 2004, **4**, 213–217.
- 12 M. Wang, J. Wang, Q. Chen and L.-M. Peng, *Adv. Funct. Mater.*, 2005, **15**, 1825–1831.
- 13 J. A. Rodríguez-Manzo, M.-S. Wang, F. Banhart, Y. Bando and D. Golberg, *Adv. Mater.*, 2009, **21**, 4477–4482.
- 14 M. Terrones, F. Banhart, N. Grobert, J.-C. Charlier, H. Terrones and P. M. Ajayan, *Phys. Rev. Lett.*, 2002, **89**, 075505.
- 15 S. H. Tsai, C. T. Shiu, W. J. Jong and H. C. Shih, *Carbon*, 2000, **38**, 1879–1902.
- 16 J. Li, C. Papadopoulos and J. Xu, *Nature*, 1999, **402**, 253.
- 17 G. Meng, Y. J. Jung, A. Cao, R. Vajtai and P. M. Ajayan, *P. Natl. Acad. Sci. USA*, 2005, **102**, 7074–7078.
- 18 C. Papadopoulos, A. Rakitin, J. Li, A. S. Vedenev and J. M. Xu, *Phys. Rev. Lett.*, 2000, **85**, 3476–3479.
- 19 H. Kohno, T. Komine, T. Hasegawa and S. Ichikawa, *Nanoscale*, 2013, **5**, 570–573.
- 20 In the origami mechanism, carbon interstitial atoms at octahedral sites in a γ -Fe catalyst nanoparticle are expelled mainly along four $\langle 112 \rangle$ directions on the four $\{111\}$ planes to form a nanotube with its axis along the $[001]$ direction of the Fe nanoparticle. The four $\{111\}$ planes/ $\langle 112 \rangle$ directions converge; therefore there are two directions of flattening. When one of the two directions is superior, a nanoribbon is formed. If the superiority changes, then the flattening direction switches to a right angle, which yields a nanotetrahedron at the switching point.
- 21 The carbon nanostructures were mounted on a TEM microgrid with a carbon membrane, and observed using a Jeol JEM2010 TEM (operated at 160 kV) and an FEI TechnaiG20 TEM (operated at 200 kV).
- 22 D. V. Kosynkin, A. L. Higginbotham, A. Sinitskii, J. R. Lomeda, A. Dimiev, B. K. Price and J. M. Tour, *Nature*, 2009, **458**, 872–877.
- 23 L. Jiao, L. Zhang, X. Wang, G. Diankov and H. Dai, *Nature*, 2009, **458**, 877–880.
- 24 A. L. Elías, A. R. Botello-Méndez, D. Meneses-Rodríguez, V. Jehová González, D. Ramírez-González, L. Ci, E. Muñoz-Sandoval, P. M. Ajayan, H. Terrones and M. Terrones, *Nano Letters*, 2010, **10**, 366–372.
- 25 K. Kim, A. Sussman and A. Zettl, *ACS Nano*, 2010, **4**, 1362–1366.
- 26 A. G. Cano-Márquez, F. J. Rodríguez-Maías, J. Campos-Delgado, C. G. Espinosa-González, F. Tristán-López, D. Ramírez-González, D. A. Cullen, D. J. Smith, M. Terrones and Y. I. Vega-Cantú, *Nano Letters*, 2009, **9**, 1527–1533.